Available online at www.sciencedirect.com

ScienceDirect

Procedia Engineering 116 (2015) 436 – 445

Procedia Engineering

www.elsevier.com/locate/procedia

8th International Conference on Asian and Pacific Coasts (APAC 2015)

Swash seepage velocity estimation using image analysis

Xiaohu Deng[a], Haijiang Liu[a]*, Zhixuan Cheng[a], Kungpeng Wang[a]

[a] *Ocean College, Zhejiang University, 866 Yuhangtang Road, Hangzhou, Zhejiang 310058, China*

Abstract

In the swash zone, the vertical flow of water into and out of the bed is one of the factors that may affect the surface sediment transport. To understand swash zone hydrodynamics, detailed measurements of swash front velocity were obtained in the swash zone by image analysis. During wave up-rush, surface water, in general, infiltrates generally perpendicularly into the beach and deflects direction when reaching groundwater table. Swash velocity plays a significant role in the up-rush infiltration process, which can be divided into three stages and positively related to the surface infiltration. As for the subsurface infiltration rate, it decreases rapidly and reaches a steady rate at the end. It is confirmed that swash front velocity can modify the infiltration process and its influence decreases towards the up-rush end. Calculated infiltration rates after incorporating the influence of swash front velocity into Darcy's law fit closely with the measurements.

Peer- Review under responsibility of organizing committee , IIT Madras , and International Steering Committee of APAC 2015

Keywords: Swash zone; Surface infiltration; Subsurface infiltration; Swash front velocity; Image analysis

1. Introduction

In the swash zone, the vertical flow of water into and out of the bed, as well as swash velocity is one of the factors which may affect the surface sediment transport (Butt et al., 2001). There exist a few infiltration models, but none is proved to be so valid (Packwood, 1983; Kang and Nielsen, 1996; Cartwright et al., 2002). At the same time, the

* Corresponding author. Tel.: +86-571-88206661; fax: +86-571-88206661.

E-mail address: haijiangliu@zju.edu.cn

Peer- Review under responsibility of organizing committee , IIT Madras , and International Steering Committee of APAC 2015
doi:10.1016/j.proeng.2015.08.309

seepage flow velocity can not be quantitatively obtained by traditional approaches. Hence, comparing to the surf zone, swash zone hydrodynamics are relatively poorly understood due in part to the difficulties of data acquisition, which makes data analysis and critical comparisons between theory and observations becoming difficult (Hughes and Baldock, 2004). As a result, there are very limited data on swash zone fluid velocities, and only one previous study compared field observations (from a gently sloping dissipative beach) with theoretical calculations (Raubenheimer, 2002).

The objective of this study is to develop a data collection and analyzing technique based on image analysis to estimate the subsurface seepage velocity in a manner that is both time- and cost-effective, and with acceptable levels of accuracy. To a certain extent, it may throw light on the infiltration process and enable us to build up a new view on sediment transport in the swash zone.

2. Experimental setup

Laboratory experiments were carried out in a water tank which consists of a 6.5m long, 0.4m high, and 0.2m wide, transparent PVC (polyvinyl chloride) flume with a 1.5m water reservoir at one end (Fig. 1). The reservoir is fronted by a gate which can be rapidly raised to produce a large plunging wave leading to a bore which propagates towards beach located downstream (Kikkert et al., 2012; Liu et al., 2015). The camera used in this experiment is the digital camera EOS 60D fixed on a triopod recording the experimental process. The camera recorded the infiltration process with a rate of 25 fps. Two spot lights were used to guarantee enough light for legible images. Experiments were conducted for a permeable beach with median diameter of sediments 1.3mm, density 2.63 g/cm^3, and porosity 0.41. The beach has a trapezoid shape with 0.3m in length on the top and 2.5m in length on the bottom and 0.34m in height. The beach slope is 12°. The initial water depth in the reservoir is 30cm and the water depth in front of the gate is 5 cm. The x-z coordinate system is settled based on the images with x-axis parallel to the bottom of the water tank and z-axis vertical to that (indicated in Fig. 3). The swash front velocity is defined as the swash tip flow velocity, parallel to the beach face. Red and blue inks were added on the beach face before experiment. They infiltrate together with water during the swash up-rush to show the percolation process and its direction. Measurements were triggered at the moment of gate opening. Time “zero” is set as the instant when the swash tip reaches the beach toe. According to experiments, the swash up-rush duration is 1.6s.

3. Methodology

To avoid the interference from equipment, image analysis was used to obtain data. The image analysis was carried out in two stages. At the first stage, images are taken at a rate of 25 fps recording the infiltration process during up-rush. Considering that grayscale values in one image differ from those in the successively recorded one, all the images can function as background values giving the initial state information. By subtracting the adjacent images, the region with the same grayscale values is black indicating no changes while region with different grayscale values will show brightness indicating wetting front or surface water elevation (Fig. 2). At the second stage, several representative points in images were selected and surface/subsurface infiltration rate and swash front velocity were evaluated. After the infiltration direction is determined, swash seepage velocity can be estimated since the time duration is recorded by images and the distance between two infiltration lines (instantaneous wetting

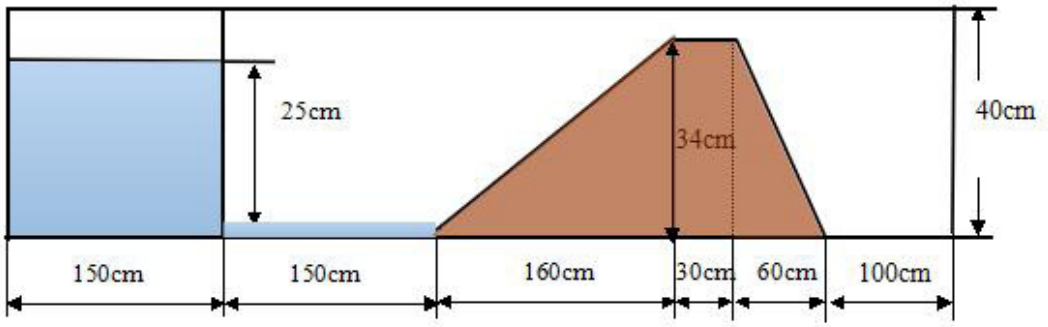

Fig. 1. Schematic diagram of experimental setup.

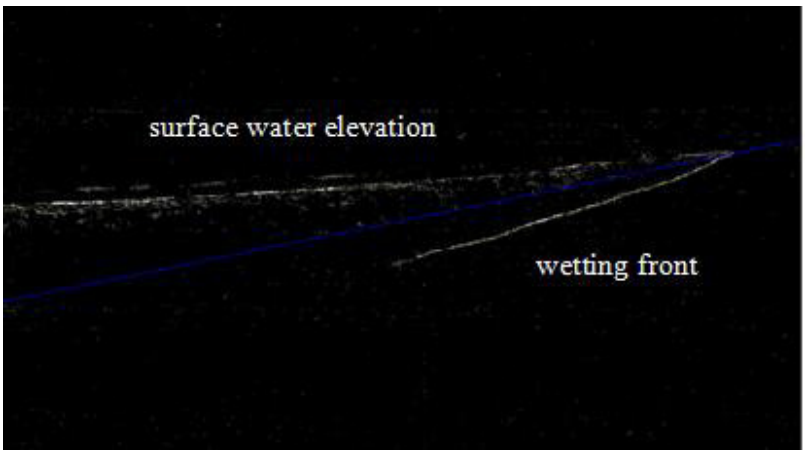

Fig. 2. A typical image showing the surface water elevation and seepage wetting front obtained from subtraction of two successive images at the run-up limit. The blue line represents the sandy beach.

fronts) can be obtained from images. On the other hand, swash front velocity was estimated by calculating the distance along the beach face at a 0.04s time interval.

4. Results

4.1. Infiltration direction

Before the experiments, blue and red inks were laid at two different positions on the beach face, respectively. During the up-rush, diffusion of these inks clearly indicates the infiltration direction (Fig. 3). However, some differences lie between these two indicators. The red ink shows that the infiltration direction is almost perpendicular to the beach face. As for the blue ink, it lies closer to the groundwater table. At the beginning, it flows perpendicularly to the beach face, then deflects to move along the groundwater table indicating a horizontal infiltration. One point to note is that the condition of waves and the saturation degree of the sand may have effects

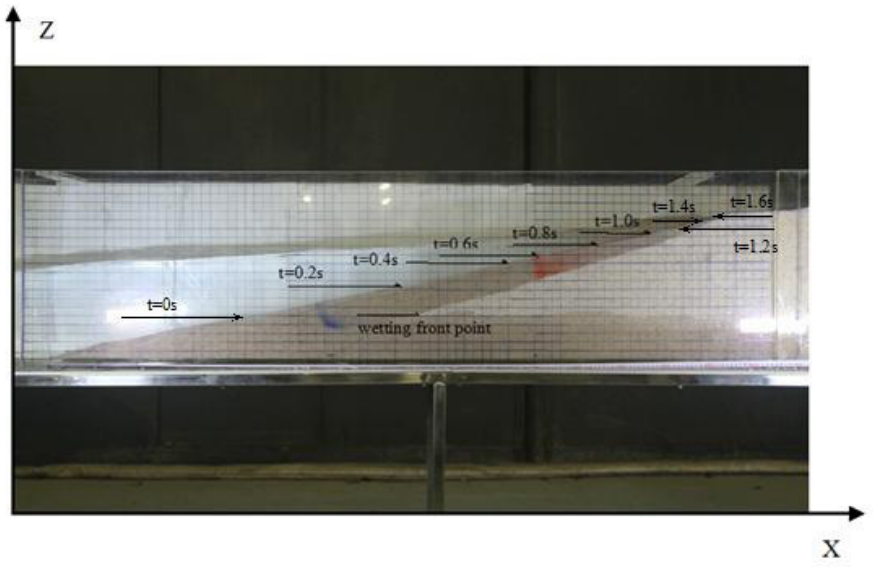

Fig. 3. Infiltration direction in the up-rush phase indicated by the red and blue inks, and time course of swash front indicated by arrows

on the infiltration direction. In this study, we focus on the infiltration process in unsaturated dry beach above the bottom groundwater table. Hence, the infiltration direction is considered to be perpendicular to the beach face.

4.2. Swash front velocity

Swash front velocity (shoreline moving velocity) represents the maximal velocity of the swash water body, and is related to the bed shear stress which has a direct impact on sediment movement. It is affected by many factors of which the water head in the reservoir and the distance between front gate and sandy beach play an important role. Fig. 4 shows the time series of swash front velocity estimated using image analysis. Three different stages can be identified during the whole swash up-rush process. At the first stage (from t=0 to 0.5s), as the swash front reaches the beach toe, the swash front velocity is the largest and decreases gradually to zero. This swash front velocity is caused by dam-breaking as the potential energy of the swash water body turns into kinematic energy. However, interference of large turbulence induced by plunging wave may affect the infiltration process. At the second stage (from t=0.5 to 1.0s), the swash water body almost uniformly climbs the beach making the water surface elevate equally. At the same time, bore is generated moving on the water surface. Both cause the swash front to propagate forwardly. Therefore, swash front velocity is still considerable large. At the third stage (from t=1.0 to 1.6s), the swash water body gradually cease moving and water surface elevation is laggardly lifted up. Bore plays an important role in making the swash front continue to climb the beach.

4.3. Surface infiltration velocity

There are many literatures concerned about infiltration, but few involves the surface infiltration velocity due to the difficulties of the data acquisition through traditional approaches. However, the sediment movement is directly related to the surface infiltration. Therefore, careful attention should be paid to it.

Comparing with swash front velocity, it can be seen that the surface infiltration and swash front velocity have the same variation tendency. The correlation coefficient is found to be 0.87 by calculating the two lines, which demonstrate the swash front velocity may have a certain impact on the infiltration process. Thus, according to Fig.5,

the surface infiltration can also be divided into three stages. At the first stage (from t=0 to 0.4s), the surface infiltration rate is much larger than the other two stages. At the second stage (from t=0.4 to 1s), the water head elevating uniformly. The slope between surface water and beach face is almost uniform during this stage, while bore moves on the water surface. Thus, water infiltrates steady with a small variation. At the third stage (from t=1.0 to 1.6s), the surface infiltration is mainly influenced by bore.

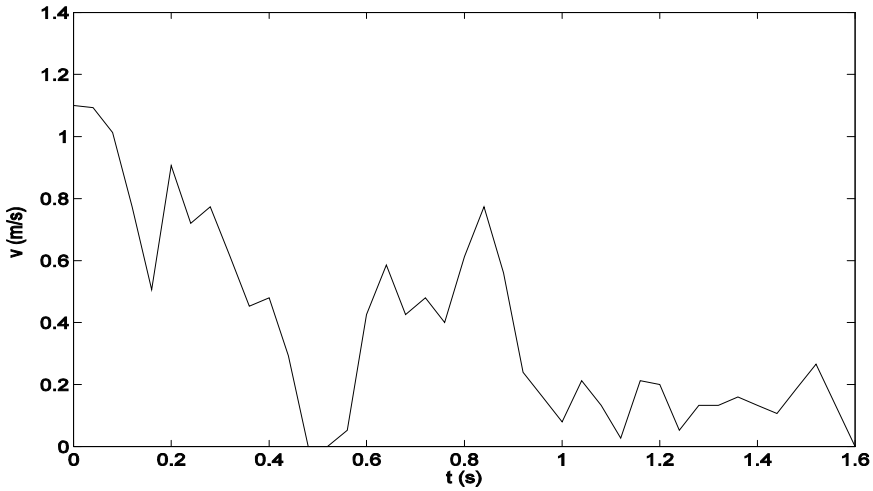

Fig. 4. Measured swash front velocity based on image analysis

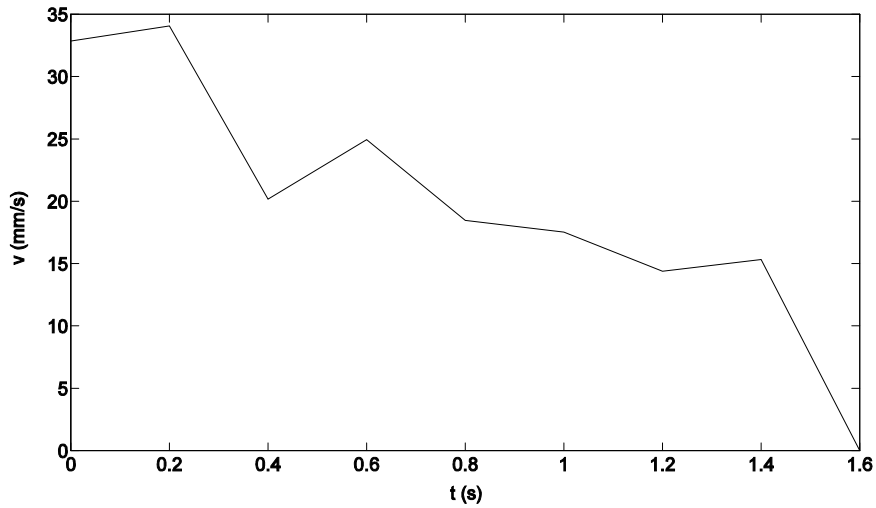

Fig. 5. Measured surface infiltration velocity based on image analysis

4.4. Subsurface infiltration velocity

In this paper, the subsurface infiltration rate is defined as the rate along the infiltration direction at a particular point from the time swash touches this point to the time of up-rush end. In Fig. 6, there are five lines with starting point at t=0.2s (position x=882mm), 0.4s (x=1096mm), 0.6s (x=1150mm), 0.8s (x=1327mm), 1.0s (x=1454mm), indicating the particular instant when swash reaches the corresponding position and infiltration process begins. It can be seen that when water infiltrates towards the inner part of the sand, though the infiltration rates of different points are different, all of them decrease rapidly and approach at a uniform rate of 13-15mm/s in the end. It takes a longer time for the lower position (e.g., x=882mm) in the sandy beach to reach the steady state. At the first stage of swash up-rush, water head changes rapidly, which causes rapidly change in infiltration rate at x=882mm, 1096mm, 1150mm. At the third stage, the swash water body almost ceases moving, and the angle between surface water and sandy beach remains the same. Subsequently, the infiltration rate is maintained at 13-15mm/s.

As in common sense, infiltration is mainly affected by the surface water head. In numerical simulation of infiltration, it usually assumes a laminar flow state and applies the Darcy's law,

$$\frac{w}{k} = -\frac{dh}{dz} \tag{1}$$

where w is the infiltration rate, k is the hydraulic conductivity, assuming to be 10mm/s, coinciding with the experimental measurements of Steenhauer (2011) with almost the same sediment size, dh is the water head loss along the infiltration distance of dz and both can be captured from images.

Fig. 7 shows the subsurface infiltration rate at x=882mm, 1096mm, 1150mm. The solid line represents the measured infiltration rate based on image analysis and the dashed line represents the infiltration rate calculated using Eq. (1). At the end of the infiltration process (t>1s), the infiltration rates of solid and dashed lines are almost the same, which indicates that the subsurface infiltration is predominantly affected by the surface water head at this stage. Nevertheless, at the initial stage (t<1s), calculated infiltration rate is smaller than the measurement, which reveals that besides the surface water head influence, there exists other mechanism to drive the subsurface infiltration process in the swash up-rush. Considering that large swash front velocity may change physical state of the beach sand, making sand texture become loose and promoting the infiltration rate, especially at the beginning of infiltration process and within top layer of the beach. In this study, we argue that the difference between the me-

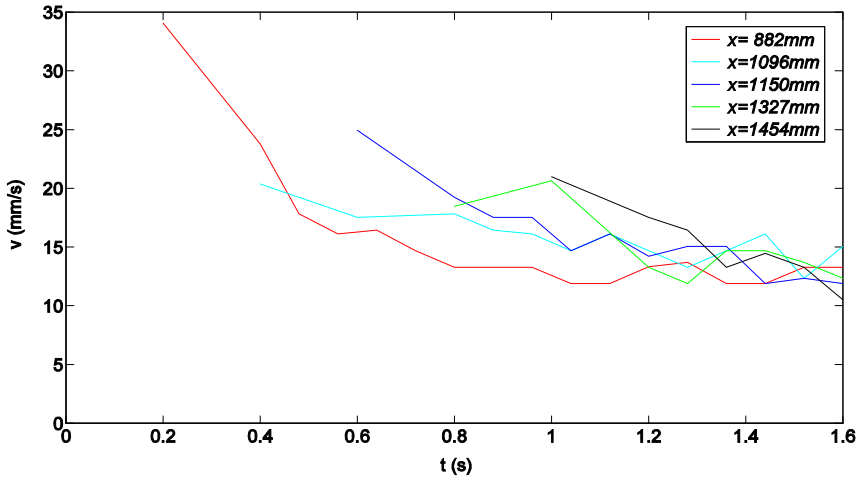

Fig. 6. Estimated subsurface infiltration velocity at five representative positions.

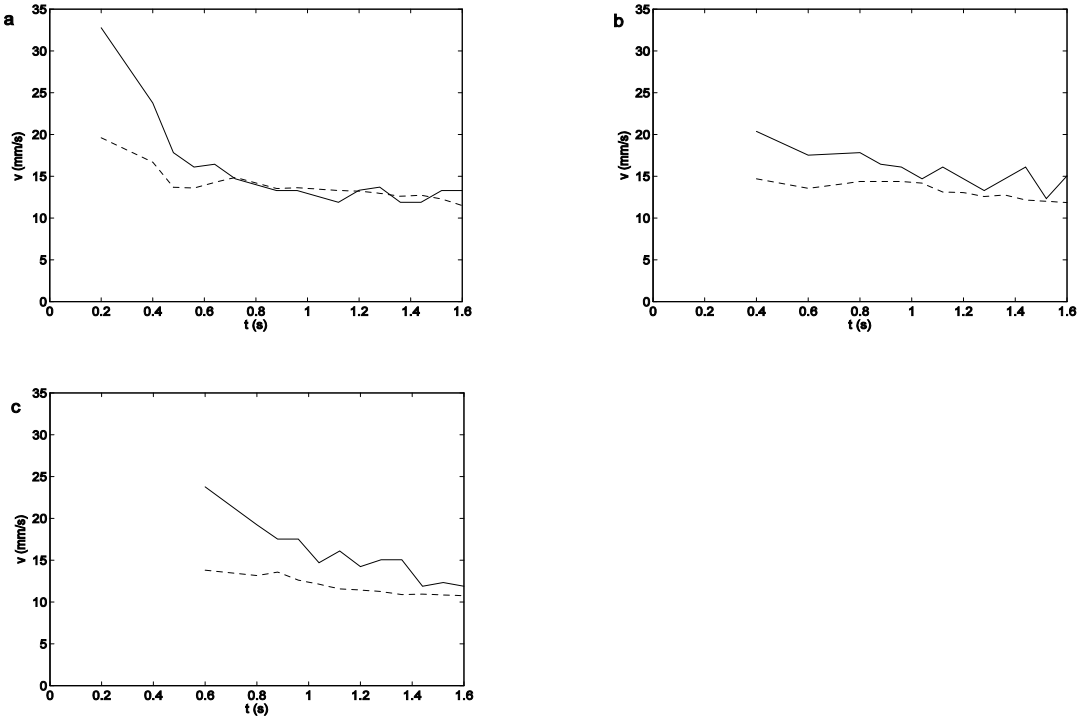

Fig. 7. Comparison between infiltration rate of the measured results (solid lines) and predicted results using Eq. (1) (dashed lines) at three different position of (a) x=882mm, (b) x=1096mm, (c) x=1150mm.

asured and calculated infiltration velocities at the initial stage may be ascribed to the influence from the swash front velocity, which will be further discussed in the following context.

5. Discussion

The spatial variation of the whole water head is the main driving mechanism for infiltration. The whole water head consists of three components. The first is the position potential energy *z* relative to the reference position; the second is the pressure potential energy *h* (temporal water head). The third is the kinematic energy ($v^2/2g$), which provides the energy for the flow to run-up. In general, the kinematic energy is neglected, and the remaining two energy components, i.e., *(h+z)*, are used for calculating the infiltration rate based on Darcy's law.

Taking the swash front velocity into consideration and considering the total water head *H* is the summation of the position head *z*, the pressure head from water body h, and the head from water movement $v^2/2g$.

$$H = h + z + \frac{v^2}{2g} \tag{2}$$

Then, the infiltration velocity is estimated based on the Darcy's law

$$\frac{w}{k} = -\frac{dH}{dz} = \alpha \frac{h + z + v^2/2g}{z} \tag{3}$$

Parameter *a* is the energy dissipation coefficient, representing the loss of the total water head. And it is found to be 0.6 in this study. During the infiltration process, it is found that the infiltration velocity in top layer of the beach is almost the same as the swash front velocity. On the other hand, water head at the wetting front is not zero though it is the boundary of dry and wet sand, as there exists infiltration velocity representing the velocity head and the air is compressed below the wetting front representing the pressure head (Steenhauer 2011).

Fig. 8 shows the comparison of surface infiltration velocity. The dots represent the measured infiltration rate based on image analysis. The solid line represents the calculated result based on Eq. (3) while the dotted line represents the infiltration rate based on Eq. 1 which doesn't take the swash front velocity into consideration. It clearly shows that the calculated results after considering the swash front velocity effect agree well with the measurements. It is not appropriate to neglect the influence of swash front velocity on infiltration at least at the beginning stage of swash up-rush. At the end of up-rush, the swash front velocity becomes small, thus, they almost coincide with each other.

Apparently, the swash front velocity is raised from the water head and plays a role in promoting infiltration, making more water penetrate into the sandy beach. This can explain the reason that in numerical simulation of Packwood (1983), the simulated run-up limit exceed the measurement while the volume of water infiltrated into b-

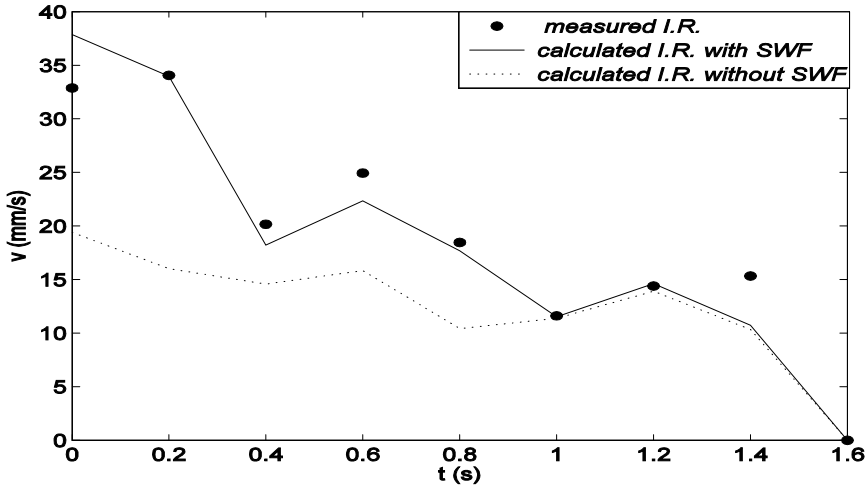

Fig. 8. Comparison between infiltration rate of measurements using image analysis (dots) and calculation based on Eq. (3) (solid line), as well as calculation based on Eq. (1) (dotted line)

each is much less than measurement since the influence of swash front velocity is not considered. Therefore, when calculating infiltration, swash front velocity should be taken into consideration.

6. Conclusion

In this study, different from the traditional research approaches applied in swash zone, image analysis was used to estimate infiltration direction and rate in the swash up-rush phase. Main conclusions drawn from this study are summarized as follows,

1. In the swash up-rush phase, subsurface infiltration is not in the vertically downward direction, but is perpendicular to the beach face. When the seepage wetting front touches the bottom groundwater table, seepage flow direction deflects to move along the groundwater table indicating a horizontal infiltration process within the groundwater.

2. Both swash front velocity and surface infiltration velocity can be divided into three different stages and a positive correlation was found between them.

3. As for the subsurface infiltration velocity, it decreases rapidly and reaches a steady rate at the up-rush end.

4. Different from the traditional understanding that subsurface infiltration has no relation with the surface wave movement. It is confirmed that swash front velocity plays an important role in infiltration process. The calculated infiltration rate containing the influence of swash front velocity agrees well with measurement. Therefore, when adopting Darcy's law for calculating the infiltration velocity in the swash up-rush, the water head should be modified to account for the effect not only from position and pressure heads but also from swash front velocity.

Acknowledgements

This study was financially supported by the Natural Science Foundation of Zhejiang Province (No. LR14E090002).

References

Butt, T., Russell, P., Turner I., (2001). The influence of swash infiltration-exfiltration on beach face sediment transport: onshore or offshore? Coastal Engineering **42**: 35-52.

Cartwright, N., Nielsen, P., Jessen, O. Z., (2002). Swash zone and near-shore watertable. Coastal Engineering.

Hughes, M. G., Baldock, T. E., (2004). Eulerian flow velocities in the swash zone: Field data and model predictions. Journal of Geophysical Research **109**(C8).

Hughes, M. G., Masselink, G., Brander R. W., (1997). Flow velocity and sediment transport in the swash zone of a steep beach. Marine Geology **138**: 91-103.

Kang, H. Y., Nielsen, P., (1996). Watertable dynamics in coastal areas. Coastal Engineering: 4601-4612.

Kikkert, G. A., O'Donoghue, T., Pokrajac, D., Dodd, N., (2012). Experimental study of bore-driven swash hydrodynamics on impermeable rough slopes. Coastal Engineering **60**: 149-166.

Liu, H., Cheng, Z., Wang, J. (2015). An experimental study on the seepage process in the swash zone. Proceedings of Coastal sediments' 15, San Diego, USA, accepted.

Nielsen, P., 1998. Coastal groundwater dynamics. Proc. Coastal Dynamics '97, ASCE, 546-555.

Packwood, A. R., (1983). The influence of beach porosity on wave uprush and backwash. Coastal Engineering **7**: 29-40.

Raubenheimer, B., (2002). Observations and predictions of fluid velocities in the surf and swash zones. Journal of Geophysical Research **107**(C11).

Steenhauer, K., Pokrajac, D., O'Donoghue, T., Kikkert, G. A., (2011). Subsurface processes generated by bore-driven swash on coarse-grained beaches. Journal of Geophysical Research **116**(C4).